CHAPTER 40

Hybrid Spectral Element Methods for Flows Over Rough Walls

Ron Henderson*
George Em Karniadakis*

Abstract. In this paper we present a new formulation for coupling spectral element discretizations to finite-difference and finite-element discretizations addressing flow problems in very complicated geometries. A general iterative relaxation procedure is employed that enforces C^1 continuity along the patching interface between the two differently discretized subdomains. In fluid flow simulations of transitional and turbulent flows the high-order discretization (spectral element) is used in the outer part of the domain where the Reynolds number is effectively very high. Near "rough" wall boundaries (where the flow is effectively very viscous) the use of low-order discretizations provides sufficient accuracy and allows for efficient treatment of the complex geometry. An analysis of the patching procedure is presented for elliptic problems and extensions to incompressible Navier-Stokes equation are implemented using a high-order splitting scheme. Several examples are given for model problems and performance is measured on both serial and parallel processors.

1. Introduction. Over the last two decades, a large number of numerical techniques have been proposed for the solution of the incompressible Navier-Stokes equations. Although the differences among these discretization techniques might have initially been very clear, there has been an increasing trend (especially this past dacade) towards construction of hybrid algorithms with components that exhibit different properties but typically share a common root. A typical example of such a confluence of numerical algorithms is the spectral element method [7], [4] which is based on two weighted-residual techniques: finite element and spectral methods. The combination of spectral-like accuracy with the flexibility in handling complex geometries have made the method quite succesfull in a number of applications in fluid dynamics, including flows in the transitional and turbulent regimes [3]. However, a straightforward application of

* Department of Mechanical and Aerospace Engineering and Program in Applied and Computational Mathematics, Princeton University, Princeton, NJ 08544

the method in simulating turbulent flows with a very strong disparity in length scales (e.g. fluid flows over arbitrarily roughened surfaces) is prohibitively expensive as the small-scale geometric irregularity imposes severe constraints that result in an extremely low convergence rate for the method.

In this work, we propose a new class of efficient hybrid discretization schemes appropriate for simulating flows over walls of arbitrary roughness (see figure 1.1). The two main components of the algorithm are a high-order scheme (spectral element method) and a low-order scheme (finite-difference or finite-element method). The use of the finite-difference discretization is essential in geometries with random boundaries, where all discretization techniques based on mappings fail. The use of low-order finite elements can also be useful in a wider class of applications incuding, for example, flows in unbounded domains, flows over surfaces with distrubuded roughness elements, etc. A new general iterative relaxation procedure is applied to allow coupling of two fundamentally different discretizations. In particular, the first component of the hybrid algorithm (spectral element method) is applied to the outer large-scale domain Ω_1, where the effective local Reynolds number is large and thus the spectral-like dispersive properties of the method are effectively utilized. In the near-wall region where an almost laminar flow prevails the second component (a low-order finite difference method) is applied providing sufficicient resolution to simulate the viscous flow and account for the small-scale irregularity of the domain Ω_2. As regards time discretization, a high-order splitting scheme [5] is employed that reduces the problem into solving a series of coupled hyperbolic and elliptic problems. Continuity of the solution along the spectral element-finite difference interface (boundary Γ in figure 1.1) is then imposed by requiring continuity of the elliptic components; the latter is accomplished using the iterative "Zanolli" patching procedure and appropriately chosen relaxation parameters [1].

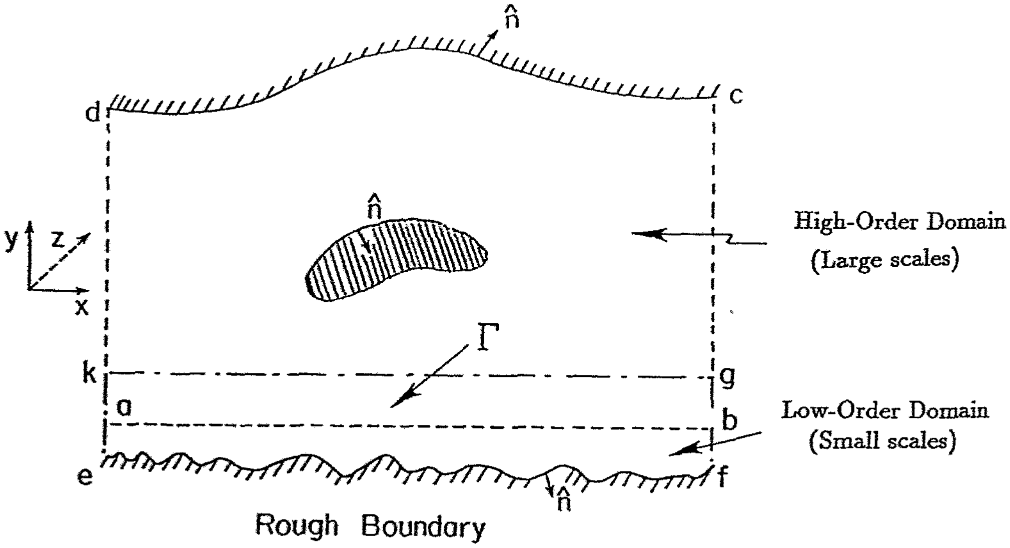

FIG. 1.1. *Geometry definition and computational subdomains for the model flow problem.*

The "Zanolli" patching procedure has been practiced in the past only in the context of similar discretizations on both domains (i.e. spectral collocation, [1]). It basically consists of solving a Dirichlet elliptic problem in domain Ω_1 and subsequently providing a pointwise flux (Neumann) condition for the solution of the corresponding elliptic problem in domain Ω_2; this procedure is then repeated until continuity of the two solutions at the interface is achieved. Convergence to the exact solution is typically obtained after three to five iterations depending on the problem size and the value of the relaxation parameter. In the current work, we have modified this patching procedure to first accomodate dissimilar discretization schemes across the two domains, and second to allow for a parallel implementation; the latter can be achieved by appropriately modifying the flux condition of the Neumann elliptic problem.

The paper is organized as follows: In section 2, we present the patching algorithm in its sequential form and subsequently introduce modifications that allow parallel implementation. Convergenece error analysis and numerical tests are presented for mixed spectral element/finite-difference discretizations of elliptic problems. In section 3, we extend the algorithm to the incompressible Navier-Stokes equations by employing a recently proposed high-order splitting scheme. We then apply the hybrid scheme to non-conforming spectral element simulation of an exact Navier-Stokes solution where the spectral (exponential) convergence is verified; subsequently a time-dependent flow example is simulated in an irregular domain. A brief discussion and conclusions are summarized in section 4.

2. Iterative Patching Procedure. Here we consider techniques for solving a general second-order elliptic partial differential equation where the gobal domain Ω is subdivided into a number of smaller, non-overlapping domains Ω_i. The emphasis is on generality in the discretizations within each subdomain and the ability, in the context of parallel computers, to update each subdomain simultaneously. Although for "conforming" discretizations (i.e. the same discrete representation of the solution in each subdomain) direct methods are still possible, in the case of fundamentally different discretizations we are forced to consider iterative procedures. One such method is that proposed in [1] and referred to here as "Zanolli" patching. The method consists of solving a sequence of alternating Dirchlet/Neumann problems, maintaining C^1 continuity and relaxing interface values to achieve C^0 continuity to within some pre-defined tolerance. As shown in [1], this procedure results in very fast convergence for the case of spectral collocation within subdomains. Here, it will be shown to perform equally well for mixed discretizations (spectral/finite difference). Also, because the original procedure is inherently serial , modifications to allow for parallel execution of the algorithm will be examined.

2.1. Sequential Algorithm. Consider the solution of the Helmholtz equation in one dimension, given by:

$$\begin{aligned} \phi_{xx} - \mu^2\phi &= f(x) \\ \phi(a) &= 0 \\ \phi(b) &= 0 \end{aligned} \tag{2.1}$$

The global domain $\Omega(a,b)$ is now subdivided into two domains, $\Omega_1(a,\delta)$ and $\Omega_2(\delta,b)$ where δ is the location of the interface or "patch". The Zanolli patching procedure is applied as follows: we look for a sequence of functions $\phi_1^n \in \Omega_1$ and $\phi_2^n \in \Omega_2$ which satisfy the following:

$$\left\{\begin{array}{rll} \phi^n_{1,xx} - \mu^2\phi_1^n & = f & in\ \Omega_1 \\ \phi_1^n(a) & = 0 & \\ \phi_1^n(\delta) & = \lambda^n & \end{array}\right. \tag{2.2}$$

$$\left\{\begin{array}{rll} \phi^n_{2,xx} - \mu^2\phi_2^n & = f & in\ \Omega_2 \\ \phi_2^n(b) & = 0 & \\ \phi_{2,x}^n(\delta) & = \phi_{1,x}^n(\delta) & \end{array}\right. \tag{2.3}$$

where n denotes the iteration, λ^1 is a given real number, and subsequent λ^n's are computed as:

$$\lambda^{n+1} = \theta \cdot \phi_2^n(\delta) + (1-\theta)\cdot\lambda^n \tag{2.4}$$

In this context, θ is a *relaxation parameter* which under certain conditions guarantees that the procedure (2.2) - (2.3) will always converge. The extension to two-dimensional problems is straightforward, with λ^n being replaced by $\lambda^n(s)$ (s denotes a local coordinate system along the patch) and the Neumann condition (2.3) replaced by an equivalent normal flux balance.

One of the important results of [1] is a theoretical prediction of optimal θ's and a method for choosing θ *dynamically* so as to accelerate convergence. Defining error functions

$$\begin{array}{rll} e_1^n & = \phi_1^n - \phi_1^{n-1} & \\ e_2^n & = \phi_2^n - \phi_2^{n-1} & \\ z^n(\theta) & = \theta\cdot\phi_2^n + (1-\theta)\cdot\phi_1^n & on\ \Gamma \end{array} \tag{2.5}$$

where Γ is the line seperating the two patched regions (refer to figure 1.1). The unique real number θ which minimizes $\|z^n(\theta) - z^{n-1}(\theta)\|^2$ is given by:

$$\theta^n = \frac{(e_1^n, e_1^n - e_2^n)}{\|e_1^n - e_2^n\|^2} \tag{2.6}$$

where $(\cdot,\cdot)$ is the normal inner product in $\mathcal{L}^2$ and $\|\cdot\|$ is the associated norm.

Several examples of the performance of this algorithm for spectral collocation are given in [1], and for 1-D spectral-finite difference discretizations in [2]. Here we demonstrate its effectiveness for 2-D problems with non-conforming discretizations by solving the Helmholtz equation in a complex domain (see figure 2.1). The global domain is subdivided into two approximately equally sized subdomains and discretized using spectral elements in Ω_1 and finite differences in Ω_2. In figure 2.2 we show convergence of the solution at the interface for several values of θ, including the case where θ is updated dynamically. The performance seen here is typical, namely 5-10 iterations for convergence independent of the complexity of the the solution.

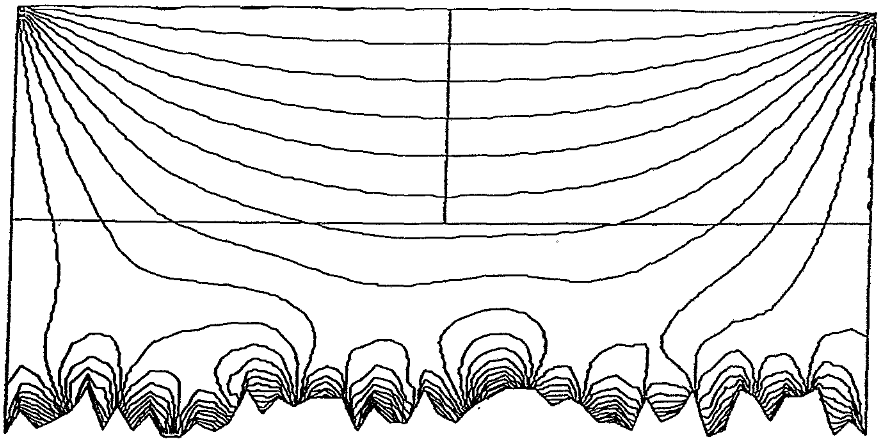

FIG. 2.1. *Simulated pressure distribution over a rough wall. The lower rectangle represents the boundary of the finite difference grid while the two upper rectangles are spectral elements. The patching procedure results in a smooth and continuous pressure distribution across the interface between the two domains.*

2.2. Parallel Algorithm. One of the drawbacks to the Zanolli procedure is that it is a "serial algorithm". Because of the coupling (through the derivative term) between (2.2) and (2.3) the solution on each subdomain must be computed in sequence, limiting the application of this procedure to sequential processing. A simple modification to (2.2) - (2.3) which allows the computations to proceed *in parallel* is:

$$(2.7)\qquad \begin{aligned} &1.\ \text{Set} \quad \begin{cases} \phi_1^n(\delta) &= \theta \cdot \phi_2^{n-1}(\delta) + (1-\theta)\cdot \phi_1^{n-1}(\delta) \\ \phi_{2,x}^n(\delta) &= \phi_{1,x}^{n-1}(\delta) \end{cases} \\ &2.\ \text{Solve} \quad \begin{cases} \phi_{1,xx}^n - \mu^2 \phi_1^n = f & \quad in\ \Omega_1 \\ \phi_{2,xx}^n - \mu^2 \phi_2^n = f & \quad in\ \Omega_2 \end{cases} \end{aligned}$$

Note that 1. denotes a communication and 2. a calculation step. While altering the convergence properties of the original scheme, this allows for each subdomain to be updated simultaneousely. On a medium- to fine-grained machine, it also allows each Ω_i to be distributed over an appropriate collection of processors such that domains with differing workloads may be updated in the same amount of "real" time.

Convergence of the procedure (2.7) is analyzed in [2] and only summarized here. Figure 2.3 shows convergence rates for a typical 2-D configuration for various fixed values of θ, and figure 2.4 shows the corresponding rates for the parallel procedure. Note that in the unrelaxed case ($\theta = 1$) the parallel procedure produces two uncoupled

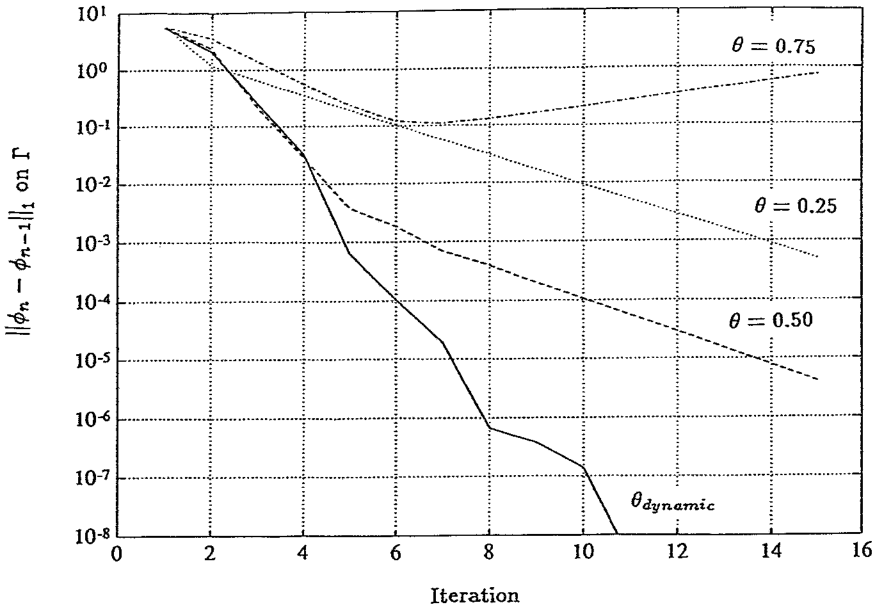

FIG. 2.2. *Interface convergence for spectral element-finite difference patching. θ refers to the relaxation parameter applied to function values along the interface.*

solutions which converge at half the rate of the serial version. However, a value of θ exists which yields acceptable convergence at better than half the serial rate. This result suggests that the amount of work represented by individual subdomains should be significant for the parallel procedure to be efficient. For efficiency measurements on typical 2-D cases the reader is referred to [2].

3. Navier-Stokes Algorithm.

3.1. High-Order Splitting Scheme. In this section, we extend the iterative patching procedure to the incompressible Navier-Stokes equations for simulations of flows in arbitrarily complex domains. The governing equations for Newtonian fluids are:

$$\begin{aligned} \frac{D\mathbf{v}}{Dt} &= -\frac{\nabla p}{\rho} + R^{-1}\nabla^2\mathbf{v} \quad in \quad \Omega \\ \nabla\cdot\mathbf{v} &= 0 \quad in \quad \Omega \end{aligned} \tag{3.1}$$

where $\mathbf{v}(\mathbf{x}, t)$ is the velocity field, p is the static pressure, R is the Reynolds number, ρ is the density and D denotes total derivative.

Numerical solution of the above system of equations will be obtained in the domains Ω_1 and Ω_2 shown in figure 1.1. Having defined the computational domain Ω we now proceed with the discretization of the system (3.1). The time-discretization employs a high-order splitting algorithm based on mixed stiffly stable schemes [5]. Considering

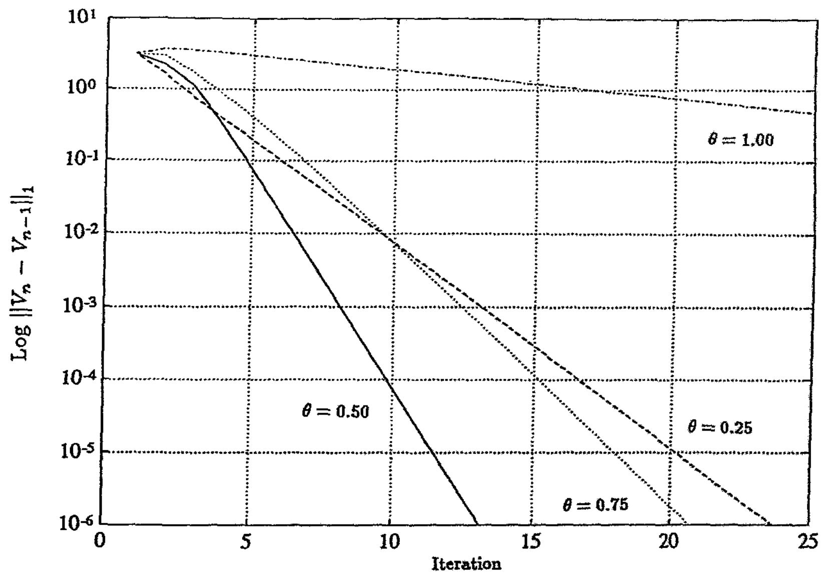

FIG. 2.3. *Spectral element-finite difference convergence rates for the sequential Zanolli patching algorithm.*

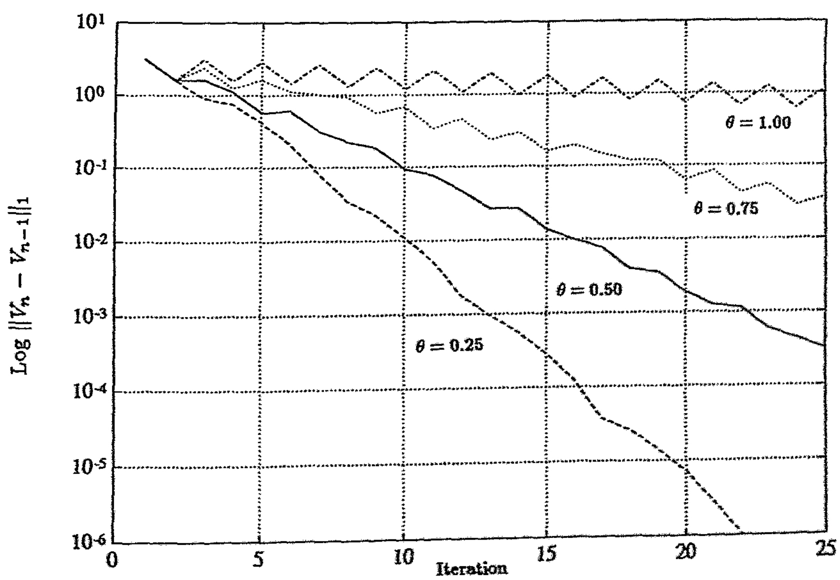

FIG. 2.4. *Spectral element-finite difference convergence for the modified (parallel) Zanolli algorithm.*

first the nonlinear terms we obtain,

$$\frac{\hat{\mathbf{v}} - \sum_{q=0}^{J-1} \alpha_q \mathbf{v}^{n-q}}{\Delta t} = -\sum_{q=0}^{J-1} \beta_q \, \mathrm{N}(\mathbf{v}^{n-q}) \tag{3.2}$$

where $\mathrm{N}(\mathbf{v}^n) = \frac{1}{2}[\mathbf{v}^n \cdot \nabla \mathbf{v}^n + \nabla \cdot (\mathbf{v}^n \cdot \mathbf{v}^n)]$ represents the nonlinear contributions written in skew-symmetric form at time level $t = n\Delta t$, and α_q, β_q are implicit/explicit weight-coefficients for the stiffly stable scheme of order J (see [5]). The next substep incorporates the pressure equation and enforces the incompressibility constraint as follows,

$$\begin{aligned} \hat{\hat{\mathbf{v}}} - \hat{\mathbf{v}} &= -\Delta t \, \nabla p^{n+1} \\ \nabla \cdot \hat{\hat{\mathbf{v}}} &= 0 \end{aligned} \tag{3.3}$$

Finally, the last substep includes the viscous corrections and the imposition of the boundary conditions, i.e.

$$\frac{\gamma_0 \mathbf{v}^{n+1} - \hat{\hat{\mathbf{v}}}}{\Delta t} = R^{-1} \nabla^2 \mathbf{v}^{n+1} \tag{3.4}$$

where γ_0 is a weight-coefficient of the backwards differentiation scheme employed [5].

The above time-treatment of the system of equations (3.1) results in a very efficient calculation procedure as it decouples the pressure and velocity equations as in (3.3) and (3.4). As regards time-accuracy of this splitting scheme a key element in this approach is the specific treatment of the pressure equation (3.3), which can be recast in the form

$$\nabla^2 p^{n+1} = \nabla \cdot (\frac{\hat{\mathbf{v}}}{\Delta t}) \tag{3.5}$$

along with the consistent high-order pressure boundary condition (see [5])

$$\frac{\partial p^{n+1}}{\partial n} = \mathbf{n} \cdot [-\sum_{q=0}^{J-1} \beta_q \mathrm{N}(\mathbf{v}^{n-q}) - R^{-1} \sum_{q=0}^{J-1} \beta_q [\nabla \times (\nabla \times \mathbf{v}^{n-q})] \tag{3.6}$$

where $\mathbf{n}$ denotes the unit normal to the boundary $\partial\Omega$. Equations (3.3) and (3.5) therefore are Poisson equations with constant coefficients; the pressure equation, for example, can be rewritten in the standard form

$$\nabla^2 \phi = g(\mathbf{x}) \tag{3.7}$$

where we have defined $\phi = p^{n+1}$, and $g(\mathbf{x}) = \nabla \cdot (\frac{\hat{\mathbf{v}}}{\Delta t})$. Standard spectral element and finite difference discretizations can then be applied in the two subdomains Ω_1 and Ω_2, while the Zanolli patching procedure is employed for both the pressure and the viscous correction terms. In this formulation (where the nonlinear terms are considered explicitly in time) the algorithms developed in the previous section are directly applicable.

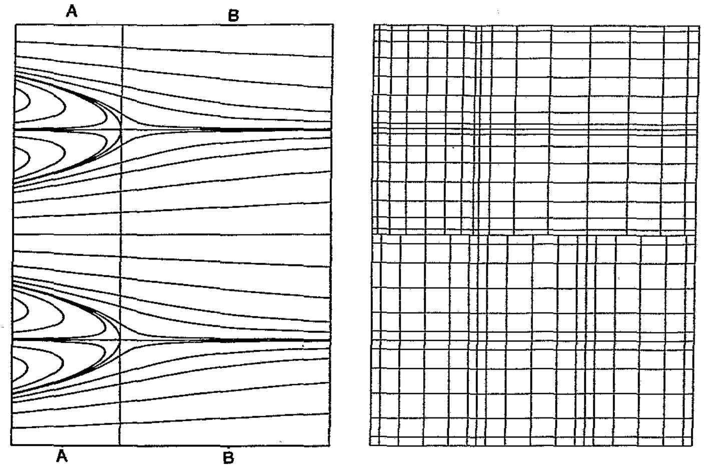

FIG. 3.1. *Streamlines and non-conforming spectral element mesh for the Kovasnay flow problem.*

3.2. Non-Conforming Spectral Elements. We now consider the solution to (3.1) where the domain Ω is subdivided into two domains Ω_1 and Ω_2 and spectral element discretizations applied in both. By applying the Zanolli patching procedure, we can relax the usual constraint of physically coincident collocation points along elemental boundaries and consider both non-conforming elements and polynomial expansions in the regions Ω_1 and Ω_2. As a test case we will solve the flow problem proposed by Kovasnay [6] where the solution is given by:

$$u = 1 - e^{\lambda x}\cos 2\pi y, \qquad v = \frac{\lambda}{2\pi}e^{\lambda x}\sin 2\pi y, \qquad p = \frac{1}{2}(1 - e^{2\lambda x}) \tag{3.8}$$

where $\lambda = R/2 - \sqrt{R^2/4 + 4\pi^2}$. This solution is shown in the form of streamlines in figure 3.1 and may represent steady, low-Reynolds number flow in the wake of a row of cylinders. The solution domain $\Omega = [-1/2, 1] \times [-1/2, 3/2]$ is subdivided into $\Omega_1 = [-1/2, 1] \times [1/2, 3/2]$ and $\Omega_2 = [-1/2, 1] \times [-1/2, 1/2]$. Within these subdomains we further subdivide the solution space into a number of spectral elements; a typical grid is shown in figure 3.1. In figure 3.2 we see that as the polynomial order N is increased simultaneously in Ω_1 and Ω_2 this nested decomposition results in *exponential* convergence both on and away from the patched interface. This convergence is critical in the case of high-order schemes as it justifies the additional work usually associated with them. Even in the case of dissimilar polynomial expansions in the two subdomains we still obtain excellent results, as shown in figure 3.3 for the particular case $N_1 = 9$ and $N_2 = 7$.

To address the issue of computational efficiency for time-dependent calculations, we simulate unsteady flow past a square cylinder in a channel with a rough wall. The computational grid is shown in figure 3.4; the boundary conditions are periodicity at inflow and outflow and no-slip along the upper and lower walls. A relatively small number of high-order spectral elements has been used to decompose the regular domain Ω_1 while a larger number of low-order finite elements have been used to represent the irregular

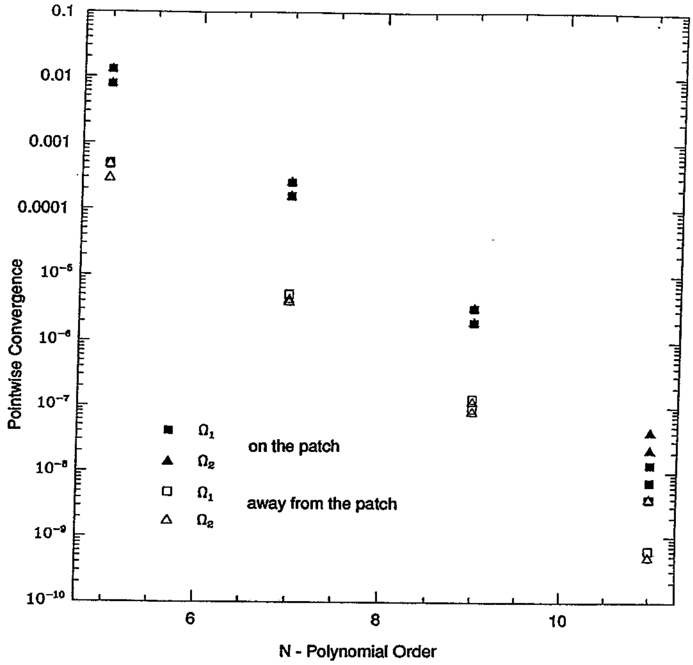

FIG. 3.2. *Convergence for the Kovasnay flow problem. As the polynomial order of the expansion within domains Ω_1 and Ω_2 is increased, we obtain exponential convergence both on and away from the patched interface.*

domain Ω_2. Again, this emphasizes the generality of the Zanolli patching procedure in resolving the two solutions. In figure 3.5 we compare fixed versus dynamic relaxation for the streamwise velocity calculations. Clearly, the fixed relaxation is inappropriate in this case but dynamic relaxation yields convergence to the tolerance of 10^{-8} in only 5 iterations per time step. A plot of streamwise velocity contours at a simulation time of $t = 153.2$ is shown in figure 3.6.

4. Discussion. We have presented a general procedure for solving elliptic problems on irregular domains using an iterative patching algorithm which allows for the coupling of fundamentally different discretization techniques. In particular, hybrid schemes which combine high-order spectral elements, finite elements, and finite difference discretizations have been formulated. Results for the Helmholtz equation were presented and performance of both serial and parallel implementations were discussed. Extension to the Navier-Stokes equations showed these results to carry through to complex numerical simulations including unsteady fluid flows.

Currently, we are working on fully parallel implementations of these algorithms as well as extending these hybrid schemes to address the issues of local refinement and composite grids, adaptive gridding, and three-dimensional flows over surfaces of arbitrary (random) roughness.

5. Acknowledgements. This work was supported by the National Science Foundation Grants CTS-8906432 and CTS-8914422, and by ONR under grant number N00014-82-C-0451. Most computations were performed on the facilities of NAS at Nasa Ames.

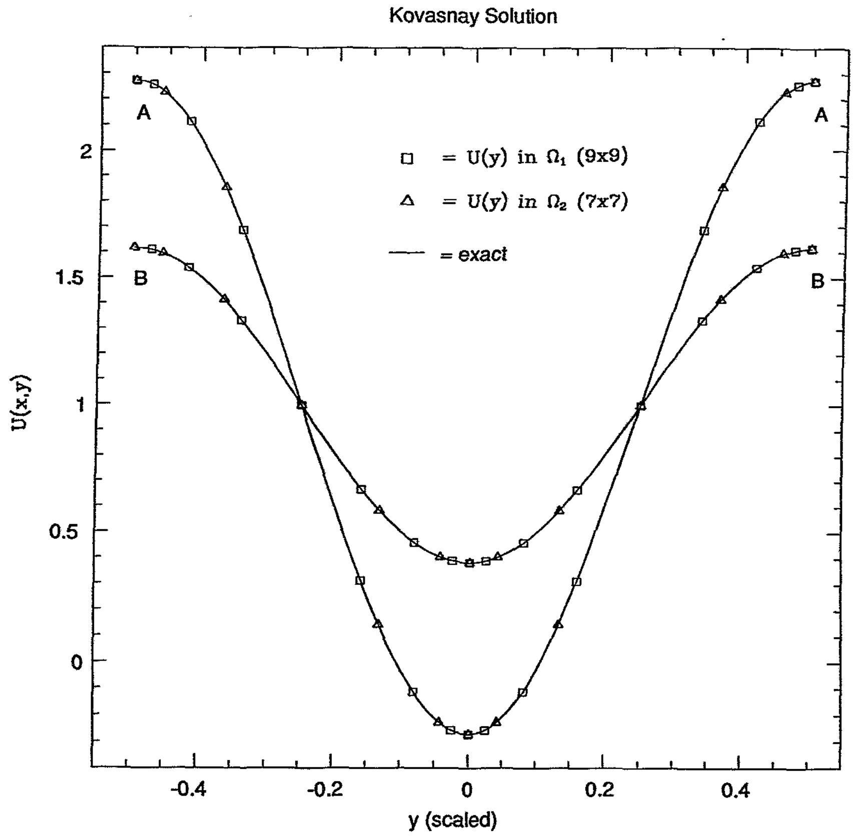

FIG. 3.3. *Profiles of the streamwise velocity component at locations $x = -0.25$ (A) and $x = 0.50$ (B) for the Kovasnay problem.*

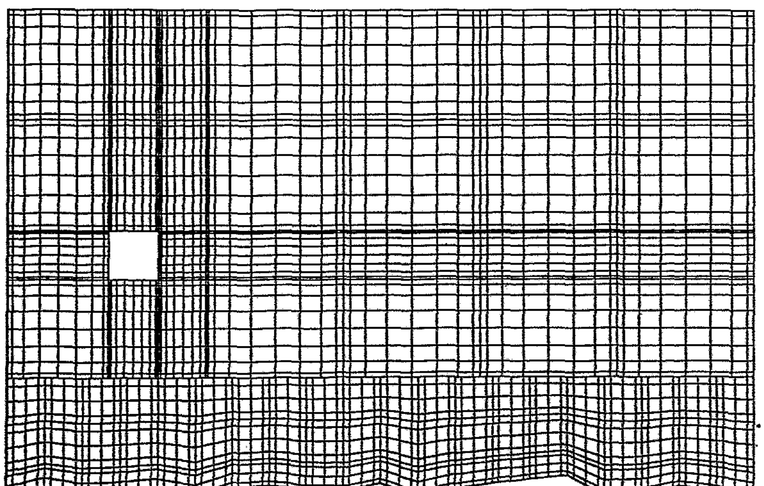

FIG. 3.4. *Non-conforming spectral element mesh for flow past a square cylinder in a channel. High-order spectral elements are used in the upper domain, while in the lower domain finite-elements provide a more efficient means of representing the irregular boundary.*

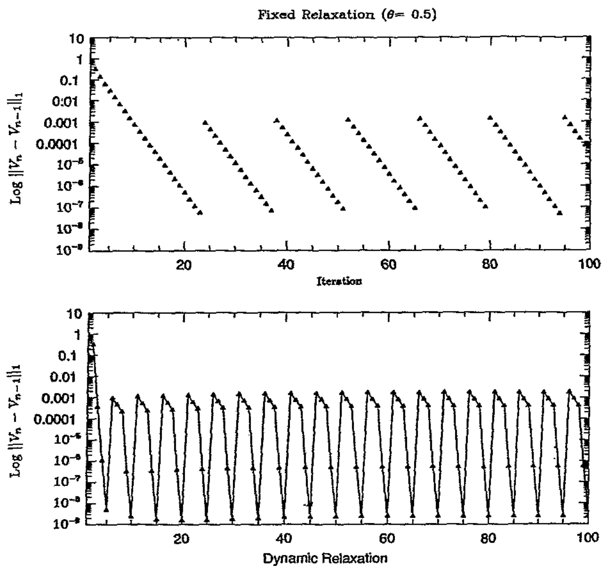

FIG. 3.5. *Convergence rates for fixed and dynamic relaxation in the streamwise velocity calculations. Over the course of 100 "global" iterations, the procedure with fixed relaxation achieves 6 time steps while the dynamically relaxed procedure achieves 20.*

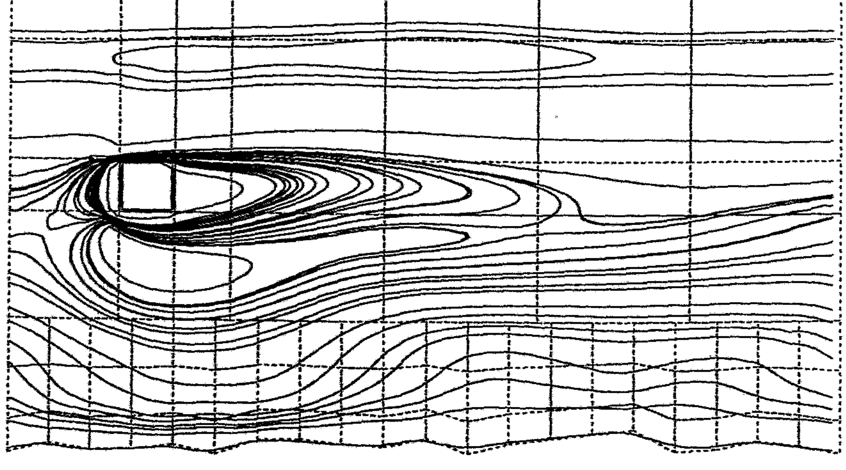

FIG. 3.6. *Streamwise velocity contours for the unsteady flow past a square cylinder at a Reynolds number of approximately 110 based on the cylinder diameter. The slightly irregular lower wall results in a flow structure much more complicated than that seen in the upper half of the channel.*

REFERENCES

[1] D. FUNARO, A. QUARTERONI, AND P. ZANOLLI, *An interative procedure with interface relaxation for domain decomposition methods*, Tech. Rept. 530, Instituto di Analisi Numerica del Consiglio Nazionale delle Ricerche, Pavia, 1985.

[2] R. HENDERSON AND G. KARNIADAKIS, *A hybrid spectral element–finite difference method for parallel computers*, in Unstructured Scientific Computations on Scalable Multi-processors, ICASE, October 1990, to appear M.I.T. Press.

[3] G. KARNIADAKIS, *Spectral element simulations of laminar and turbulent flows in complex geometries*, Applied Numerical Mathematics, 6 (1989), p. 85.

[4] G. KARNIADAKIS, E. BULLISTER, AND A. PATERA, *A spectral element method for solution of two- and three-dimensional time dependent Navier-Stokes equations*, in Finite Element Methods for Nonlinear Problems, Springer-Verlag, 1985, p. 803.

[5] G. KARNIADAKIS, M. ISRAELI, AND S. ORSZAG, *High-order splitting methods for incompressible Navier-Stokes equations*, Journal of Computational Physics, (1991). to appear.

[6] L. KOVASNAY, *Laminar flow behind a two-dimensional grid*, in Proc. Cambridge Phil. Society, 1948, p. 44.

[7] A. PATERA, *A spectral element method for Fluid Dynamics; Laminar flow in a channel expansion*, Journal of Computational Physics, (1984), p. 468.